HHS Public Access

Author manuscript

Bone. Author manuscript; available in PMC 2024 March 13.

Published in final edited form as:

Bone. 2024 February ; 179: 116983. doi:10.1016/j.bone.2023.116983.

Parathyroid hormone and trabectedin have differing effects on macrophages and stress fracture repair

Laura E. Zweifler[1], **Benjamin P. Sinder**[1], **Chris Stephan**[2], **Amy J. Koh**[1], **Justin Do**[1], **Emily Ulrich**[1], **Jobanpreet Grewal**[1], **Cecilia Woo**[1], **Lena Batoon**[1], **Kenneth Kozloff**[2], **Hernan Roca**[1], **Yuji Mishina**[3], **Laurie K. McCauley**[1,4]

[1]Department of Periodontics and Oral Medicine, University of Michigan School of Dentistry, Ann Arbor, MI

[2]Department of Orthopedic Surgery, University of Michigan, Ann Arbor, MI

[3]Department of Biologic and Materials Science, University of Michigan School of Dentistry, Ann Arbor, MI

[4]Department of Pathology, University of Michigan, Medical School, Ann Arbor, MI

Abstract

Stress fractures occur as a result of repeated mechanical stress on bone and are commonly found in the load-bearing lower extremities. Macrophages are key players in the immune system and play an important role in bone remodeling and fracture healing. However, the role of macrophages in stress fractures has not been adequately addressed. We hypothesize that macrophage infiltration into a stress fracture callus site promotes bone healing. To test this, a unilateral stress fracture induction model was employed in which the murine ulna of four-month-old, C57BL/6J male mice was repeatedly loaded with a pre-determined force until the bone was displaced a distance below the threshold for complete fracture. Mice were treated daily with parathyroid hormone (PTH, 50 μg/kg/day) starting two days before injury and continued until 24 hours before euthanasia either four or six days after injury, or treated with trabectedin (0.15 mg/kg) on the day of stress fracture and euthanized three or seven days after injury. These

Corresponding Author: Hernan Roca, University of Michigan School of Dentistry, 1011 N. University Ave., Ann Arbor MI 48109, rocach@umich.edu.

Author Contributions following CRediT roles:

Laura E. Zweifler: conceptualization, methodology, formal analysis, investigation, writing – original draft, writing – review & editing, visualization, supervision, project administration, funding acquisition
Benjamin P. Sinder: conceptualization, methodology, formal analysis, investigation, writing – original draft, writing – review & editing, visualization, supervision, project administration, funding acquisition
Chris Stephan: methodology, investigation, resources, writing – review & editing
Amy J. Koh: conceptualization, methodology, resources, writing – review & editing, supervision, project administration
Justin Do: formal analysis, investigation, writing – review & editing
Emily Ulrich: formal analysis, investigation, writing – review & editing
Jobanpreet Grewal: formal analysis, investigation, writing – review & editing
Cecilia Woo: formal analysis, investigation, writing – review & editing
Lena Batoon: methodology, resources, writing – review & editing
Kenneth Kozloff: conceptualization, methodology, resources, writing – review & editing, supervision, project administration
Hernan Roca: conceptualization, methodology, resources, writing – review & editing, supervision, funding acquisition
Yuji Mishina: conceptualization, methodology, writing – review & editing, supervision, project administration
Laurie K. McCauley: conceptualization, methodology, resources, writing – review & editing, supervision, project administration, funding acquisition

Declarations of Interest: none

treatments were used due to their established effects on macrophages. While macrophages have been implicated in the anabolic effects of PTH, trabectedin, an FDA approved chemotherapeutic, compromises macrophage function and reduces bone mass. At three- and four-days post injury, callus macrophage numbers were analyzed histologically. There was a significant increase in macrophages with PTH treatment compared to vehicle in the callus site. By one week of healing, treatments differentially affected the bony callus as analyzed by microcomputed tomography. PTH enhanced callus bone volume. Conversely, callus bone volume was decreased with trabectedin treatment. Interestingly, concurrent treatment with PTH and trabectedin rescued the reduction observed in the callus with trabectedin treatment alone. This study reports on the key involvement of macrophages during stress fracture healing. Given these observed outcomes on macrophage physiology and bone healing, these findings may be important for patients actively receiving either of these FDA-approved therapeutics.

Keywords

stress fracture; parathyroid hormone (PTH); trabectedin; bone healing; macrophage

1. Introduction

The skeletal system relies on impact and gravitational forces for optimal health, as evidenced by the loss of bone mineral density during space flight and bed rest.(1) Activity (walking, running, jumping) and gravity lead to changes in the bony architecture. Under normal conditions, bone can respond to mechanotransduction signals appropriately, resulting in maintenance of bone mass.(2) However, if the forces applied to the bone outpace the cellular ability to respond, resulting in creation or propagation of microdamage, stress fractures can occur.(3, 4) Stress fractures are especially common in athletes and military personnel who experience excessive bone loading forces, and most often occur in weight-bearing bones of the lower extremity.(5) Although wide ranges are reported in the literature, stress fractures affect up to 20% of new military recruits during basic training and account for up to 20% of sports medicine injuries.(6, 7)

Following bone fracture, there are three phases of healing: inflammation, repair, and remodeling. All three phases are important to restore the function of bone, but the inflammatory phase is a key initiator of this process.(8) During injury, blood vessel rupture signals the recruitment of immune cells and secretion of cytokines.(9) Macrophages direct the injury site through the inflammatory cascade. Following infiltration into the fracture site, they polarize to an M1-like phenotype. After clearing the area of dead cells and debris, macrophages acquire a pro-repair M2-like phenotype. During each segment, macrophages secrete key cytokines and act as regulator to the fracture microenvironment. (10, 11) Macrophage depletion has been shown to compromise endochondral models of fracture repair (12, 13) and intramembranous models of bone healing (13, 14) that disturb the macrophage-rich marrow environment. Repetitive cyclic loading of the skeleton can also stimulate a bone healing response on the periosteal surface without gross injury to the macrophage-rich marrow microenvironment, mimicking a stress fracture.(15, 16) While monocyte chemoattractant protein 1 (MCP-1) gene expression is upregulated during murine

models of stress fracture healing,(17) the presence of macrophages and their impact on this periosteal model of bone healing has not been explored.

Parathyroid hormone (PTH) is an FDA-approved bone anabolic agent that has been used since 2002 for the treatment of osteoporosis. While the exact mechanism responsible for intermittent PTH-induced anabolism is unknown, advances in studies examining PTH in genetically modified animals has generated some insight.(18) Osteoblast-lineage cells have been widely considered for this anabolic effect, but there is an increasing appreciation that PTH indirectly targets and acts on numerous other cell types including macrophages. The effects of PTH treatment in macrophage-depleted mice are dependent on the model used for depletion. In MAFIA mice, in which apoptosis of macrophages and dendritic cells is induced using the colony stimulating factor 1 receptor (Csf1r) promotor, there is a decrease in the PTH anabolic response, while in contrast clodronate liposome-induced macrophage apoptosis leads to the recruitment of more macrophages and an increase in the anabolic PTH response.(19)

Trabectedin, an FDA approved chemotherapeutic, has been shown to induce apoptosis of macrophages *in vitro* and *in vivo*, which plays a critical role in its anti-tumorigenic effects.(20) Mechanistically, trabectedin induces apoptosis in macrophages via binding to the TNF-related apoptosis-inducing (TRAIL) receptors, of which macrophages are particularly sensitive to compared to other immune cells such as T and B lymphocytes.(20) Previously, we investigated the role of ablating macrophages by trabectedin and found similar negative impacts on macrophages *in vitro*, osteal macrophages *in vivo*, and bone formation and bone mass.(21, 22)

While stress fracture healing with PTH treatment has been reported to be enhanced in rats (23) and humans,(24) the effect of macrophages has not been shown. Therefore, the objective of this study was to determine the importance of macrophages during stress fracture healing using two models. Given that PTH and trabectedin have opposing effects on macrophages in bone, and that both PTH and trabectedin are FDA approved therapies, there is strong clinical motivation to understand how these therapies may impact healing outcomes in patients at risk for fracture.

2. Materials and Methods

2.1 Mice and Stress Fracture Model

All animal experiments were performed with the approval of the Institutional Animal Care and Use Committee (IACUC) at the University of Michigan, Ann Arbor, and were conducted in accordance with ARRIVE guidelines. Male C57BL/6J mice (four month) were used. Stress fractures were induced using an established cyclic fatigue stress fracture model (16) in which 80% of the ultimate force required for complete fracture was repeatedly loaded at 2Hz with a haversine wave force using a Bose Enduratec 3200 with a 10lb load cell (Transducer Techniques MDB-10). Loading continued until the ulna displaced 60% of the total displacement needed for complete fracture. To establish baseline ultimate force and displacement, a subset of each cohort (n=2–3) was used to first determine the ultimate force under axial monotonic loading in the left forearm (4.3–4.6 N). The right forearms of these

same mice were then loaded with 80% of the ultimate force (3.4–3.7 N) until complete fracture, where displacement was recorded (0.9–1.1 mm). These mice were immediately euthanized while still under isoflurane anesthesia.

2.2 PTH Treatment

PTH (Bachem 4011474) was prepared in a sterile solution of 0.9% saline to a stock concentration of 10 μg/mL and stored at −20°C until use. Animals were treated daily with PTH (50 μg/kg) or vehicle (0.9% saline) by subcutaneous injection starting two days before induction of stress fracture and continued for four more days (six days total) or six more days (eight days total) post fracture. The PTH dose was chosen to optimize the response guided by our previous work (18). Mice were euthanized 24 hours after the final dose of vehicle or PTH.(21)

2.3 Trabectedin Treatment

Trabectedin (PharmaMar) was dissolved in dimethyl sulfoxide (DMSO) at a stock concentration of 1mM and stored at −20°C until use. Animals were treated with trabectedin (0.15mg/kg) or vehicle (0.9% saline and DMSO) by retro-orbital intravenous injection several hours after induction of stress fracture. This dose was previously established in cancer models (20) and more recently used to test changes in skeletal homeostasis.(21)

2.4 Microcomputed Tomography (microCT)

The right forearms (radius and ulna) of mice were dissected with the muscle left intact (to avoid further bone damage), immediately fixed overnight in 4% paraformaldehyde at 4°C, and stored in phosphate buffered saline (PBS) until scanned by microCT (Scanco μCT-100) at a 12 μm isotropic voxel size in agarose gel. For microCT analysis, the total volume was defined by manually outlining a region of interest encompassing the callus. A global threshold was set to 120 mgHA/cc to separate bone from background.

2.5 Histology and Macrophage (F4/80), Osteoclast (TRAP), and Osteoblast (OCN) Staining

After microCT scanning of the fixed right forearm, bones were decalcified in 14% EDTA then placed in 30% sucrose overnight. Forearms were cryo-embedded (TissueTek O.C.T) and sectioned transversely at 16–18 μm. The position of the callus was guided by the microCT scan, as well as by visual inspection of the sections. Hematoxylin and eosin (H&E) staining was performed using routine protocol.

To determine if macrophages were present in the callus, immunostaining for F4/80 was performed with a rat anti-mouse F4/80 clone CI:A3–1 antibody (Bio-Rad MCA497RT and Abcam ab6640). Briefly, for the antibody sourced from Bio-Rad (MCA497RT), samples were blocked with 5% heat-inactivated donkey serum in 1x PBS for two hours, then stained with F4/80 rat anti-mouse antibody at 1:100 dilution in blocking solution and visualized with a Cy3 goat anti-rat secondary antibody (Thermo Fisher A1434) with a 1:500 dilution. Sections were cover-slipped with Prolong Gold with DAPI and imaged on a Nikon microscope with a fluorescent source. When Abcam ab6640 was used, sections were treated with trypsin for antigen retrieval, followed by blocking with Background Sniper (Biocare Medical BS966). The primary antibody was diluted at 1:250 in DaVinci Green

Diluent (Biocare Medical PD900) and visualized with an Alexa Fluor 647 goat anti-rat secondary antibody (Biolegend 405416) using a 1:200 dilution. Sections were cover-slipped with Prolong Gold with DAPI and imaged on a Leica Thunder DMi8 microscope. Analysis was done using ImageJ (National Institutes of Health, NIH).

Osteoclasts were visualized following a tartrate-resistant acid phosphatase (TRAP) stain protocol as previously described (25) with an additional pre-incubation in 0.2 M tris hydrochloride for 1 hour at 37°C. Color variations are hematoxylin dependent.

For osteoblast detection, osteocalcin (OCN) staining was performed. Slides were subjected to antigen retrieval by warmed (37°C) proteinase K (Thermo Fisher AM2546) in TEN buffer followed by several washes with tris buffered saline (TBS). Next, blocking was performed with a 10% heat-inactivated fetal bovine serum and 10% heat-inactivated normal goat serum in TBS for one hour at room temperature. Sections were exposed to the primary antibody (rat anti-mouse osteocalcin 1:300, Thermo Fisher PA5–78870) for two hours at room temperature, followed by washes, and exposure to the secondary goat anti-rabbit Alexa Fluor 680 (Thermo Fisher A21076) antibody in a 1:200 dilution. Slides were cover-slipped with Prolong Gold with DAPI. Images were taken on a Leica Thunder DMi8 and analyzed with ImageJ.

2.6 Statistical Analysis

All data are reported as the mean ± standard deviation. Graphs are plotted with each point representing a biological replicate. Statistics were performed using GraphPad Prism 9. Treatment versus vehicle outcomes were tested using an unpaired, two-tailed t test with p set at 0.05.

3. Results

3.1 Repeated ulnar loading leads to callus formation and macrophage infiltration.

To induce a stress fracture, mice were anesthetized with isoflurane, and their right forearm was placed between a load cell and a cup (Figure 1A, B). To characterize the model and determine if macrophages were present in the callus, n=4 mice were loaded and euthanized after one week with half (n=2) embedded in paraffin (hematoxylin and eosin, H&E) and half (n=2) embedded for cryosections (immunofluorescence). H&E staining of vehicle-treated mice showed a callus of woven bone that forms around the ulna (Figure 1D, E) and is not seen in the contralateral, non-loaded ulna (Figure 1C). Macrophage staining using F4/80 showed infiltration of macrophages into the callus site (Figure 1G, H). This validated the presence of macrophages at the injury site itself following stress fracture.

3.2 PTH treatment enhances macrophage infiltration into the callus and results in increased callus bone volume following stress fracture induction.

The role of macrophages in the callus site following a stress fracture has not been reported. To prime the mobilization of macrophages, mice were treated with 50 μg/kg PTH or vehicle starting two days before stress fracture induction. Treatment continued daily until 24 hours before mice were euthanized, four days post injury (for a total of six days of PTH or vehicle

treatment) (Figure 2A). Infiltration of macrophages in the callus was significantly higher with PTH treatment as evidenced by a higher number of F4/80 positive cells relative to the callus area (PTH = 896.01 ± 215.13 cells/mm^2, vehicle = 642.10 ± 210.65 cells/mm^2, $p<0.05$, Figure 2B–D). At this early time point, bony callus formation was limited. There were no significant differences between treatment groups for callus bone volume per total volume (vehicle = 0.84 ± 0.10, PTH = 0.86 ± 0.09) or callus bone volume (vehicle = 7.14 × 10^{-4} ± 2.34 × 10^{-4} mm^3, PTH = 9.22 × 10^{-4} ± 6.48 × 10^{-4} mm^3) (Figure 2 E–H), suggesting that macrophage infiltration into the injury site precedes callus formation in response to injury.

Our next question was to understand the impact of PTH treatment on stress fracture healing at a later time point. Bony callus was evaluated six days post-injury (eight days of treatment) (Figure 3A). When samples were stained for macrophages, there was no difference between PTH (517.83 ± 199.72 cells/mm^2) and vehicle (579.80 ± 173.03 cells/mm^2) treatments on the number of F4/80 positive cells per callus area (Figure 3B–D). However, microCT analysis of the callus site showed a significantly larger BV/TV with PTH (mean = 0.63 ± 0.05) compared to vehicle (0.54 ± 0.08, $p<0.001$) (Figure 3E–G). The total bone formed in the injured ulna was also larger in mice treated with PTH (vehicle = 0.20 ± 0.10 mm^3, PTH = 0.36 ± 0.15 mm^3, $p<0.01$) (Figure 3H). At the time of euthanasia, serum procollagen type I N-terminal peptide (P1NP) was assessed as a marker of bone formation and confirmation of PTH activity. P1NP was higher in PTH treated mice (40.04 ± 17.68 ng/mL, vehicle = 23.57 ± 7.37 ng/mL, $p<0.01$) (Figure 3I).

Osteocalcin expression was examined to evaluate osteoblasts within the callus area (Figure 3J–L). PTH treatment had no impact on the osteocalcin positive area in the callus (vehicle = 1.14 ± 0.85%, PTH = 0.94 ± 1.22%). Osteoclasts were assessed within the callus by staining for TRAP and quantifying the area of the callus and TRAP-positive cells per bone surface area, but no differences were noted (vehicle = 4.98 ± 1.84 cells/mm PTH = 4.33 ± 1.31 cells/mm; Figure 3M–O).

3.3 Macrophage infiltration and callus bone volume was reduced with trabectedin treatment.

To reduce macrophage infiltration during healing, mice were treated with 0.15 mg/kg of trabectedin or vehicle on the day of stress fracture (Figure 4A). Trabectedin has been shown to be cytotoxic to mononuclear phagocytes and can induce selective macrophage depletion. (20) Although the number of F4/80 positive cells did not change when normalized to the callus area (vehicle = 127.70 ± 53.74 cells/mm^2, trabectedin = 95.03 ± 46.67 cells/mm^2; Figure 4B–D), the total number of F4/80 positive cells was significantly reduced with trabectedin treatment (vehicle = 94.00 ± 35.45 cells, trabectedin = 41.50 ± 29.14, $p<0.01$; data not shown). Contrary to the positive impact of PTH on callus bone volume, trabectedin treatment resulted in a smaller hard callus as analyzed by microCT (0.09 ± 0.05 mm^3, vehicle = 0.21 ± 0.06 mm^3) (Figure 4H). The callus BV/TV was not significantly different between the treatment groups (vehicle = 0.64 ± 0.07, trabectedin = 0.61 ± 0.10) (Figure 4E–G), suggesting that the extent of callus size, not organization of bone within, was affected by trabectedin.

3.4 PTH rescues trabectedin inhibited stress fracture healing.

Given the differing results of stress fracture healing when treated with PTH or vehicle, a cohort of mice were treated with either vehicle or PTH + trabectedin. The same regimen was followed as previously described, with PTH treatment starting two days before and trabectedin treatment started on the day of stress fracture induction (Figure 5A). After one week of healing, right ulnae were scanned by microCT (Figure 5E–H). Analysis of the callus shows that there was increased bone fraction in the callus with both PTH + trabectedin treatment (vehicle = 0.51 ± 0.07, PTH + trabectedin = 0.62 ± 0.04, $p<0.0001$) with similar values to PTH treatment alone (Figure 5G). Interestingly, serum P1NP was unchanged between the two groups (vehicle = 45.92 ± 20.90 ng/mL, PTH + trabectedin = 59.28 ± 20.55 ng/mL; Figure 5I). The osteoblasts, reported as the area of the callus fluorescently labeled with osteocalcin, and the number of osteoclasts, reported as TRAP positive cells per bone surface, were unchanged between the two treatment groups (Figure 5J–O).

4. Discussion

This study focused on the role of macrophages in bone and adds new data describing their presence and role during stress fracture repair. While significant contributions have been made highlighting the impact of macrophages in bone homeostasis and bone repair, this study is unique in several respects. First, we highlight the presence of macrophages during the stress fracture repair process. In addition, we utilize two different FDA-approved treatments to activate and target macrophages and show the resultant impact that this treatment has on bone healing. PTH treatment led to enhanced callus macrophage infiltration and greater callus bone volume. In contrast, trabectedin treatment reduced macrophage number and a smaller callus bone volume was observed. However, the macrophage ablation is resolved by administration of PTH and trabectedin.

Bone healing occurs through two mechanisms: endochondral ossification and/or intramembranous ossification. Many studies focused on long bone healing have used fixed, complete fracture models, which heal via both endochondral and intramembranous pathways.(26) Other models have been employed, such as the cortical drill hole model, to focus on intramembranous ossification.(27) Murine stress fracture models have been developed more recently, and there has been a series of work which characterizes the healing on the periosteal surface (15, 16, 28). We did not stain histological sections for chondrocytes, therefore results are limited to intramembranous bone healing models in the periosteum only.

This study highlights changes in macrophage number as a function of time during stress fracture repair. Although the effect of PTH in stress fracture healing has been studied in rats, the earliest reported results are one-week post injury, (23) making the present study novel in evaluating the mouse callus at an early time point with PTH treatment. The histological focus of this study was the evaluation of macrophages. While PTH treatment induced a significant increase in macrophages, trabectedin significantly decreased the number of macrophages in the injury site at an early time point (3–4 days post injury). Interestingly, the bony callus was not affected by PTH treatment until one week after stress fracture

induction. By that time, there was increased callus bone volume per total volume and callus bone volume in response to PTH. In contrast to the PTH treatment, trabectedin treatment significantly reduced the callus bone volume after one week, but this response was rescued by concurrent administration of both therapeutics. Neither osteoblasts nor osteoclasts were affected by PTH treatment alone or PTH and trabectedin treatment after one week of healing; however, differences may occur at other timepoints that were not evaluated. Alternatively, the activity of these cells may be altered. It is possible that other cell types, such as B cells, T cells, and osteoprogenitor cells differ in these models as well.

When interpreting this data, it is important to note how macrophage function can differ and drive healing outcomes. Macrophages exist on a continuum from M1-like, or pro-inflammatory, to M2-like, or pro-resolving, although the present study did not evaluate macrophage polarization. Macrophages infiltrating the callus of older mice , in which fracture healing is delayed, express more M1 related genes than younger mice.(28) In tibial fracture studies, Alexander et. al. have shown two distinct macrophage populations throughout bone healing: tissue-resident osteomacs and inflammatory macrophages, with osteomacs being a key contributor to collagen deposition during intramembranous ossification healing.(14) Importantly, osteomacs are also found on the periosteal surface of bone, (29) where stress fracture callus formation takes place in our model. Given this information, paired with the stress fracture model having a reduced inflammatory response, (30) fatigue loading was the optimal model to study macrophage contribution to healing. In the context of stress fractures, Coates et al. reported minimal F4/80 positive macrophage contribution to the callus. However, they observed a more robust F4/80 presence in a full fracture model (30). The disparities in our data may be attributed to different models of stress fracture induction (Coates et al. used both a smaller force and displacement) and plane of sectioning (evaluation was focused on the bone marrow space using sagittal sections as opposed to transverse, used here).

A primary function of macrophages is phagocytosis and the clearance of dead cells, which is enhanced in M2-like cells.(31) Schlundt et. al. have shown that enrichment of M2-like macrophages with interleukin 4 and 13 enhanced bone formation using a femoral fracture model.(32) PTH has been shown to increase resolvins in murine bone marrow, and macrophage treatment with resolvins enhances phagocytic activity.(33) We have previously shown that macrophages from mice treated with trabectedin had a reduced ability to phagocytose apoptotic cells.(21)

PTH has been prescribed since 2002 for the treatment of osteoporosis in patients with a high risk for fracture and has been shown to reduce the risk of vertebral and nonvertebral fractures.(34–36) Although it is currently used off-label, early evidence supports the administration of PTH for fracture healing (37–39) and there is ongoing work to evaluate PTH in stress fracture healing specifically (40). The FDA approved trabectedin in 2015 as a second-line treatment option for advanced soft tissue sarcomas.(41) It is also used for recurrent ovarian cancer treatment, (42) and is under investigation in a phase II/III trial for metastatic uterine leiomyosarcoma (NCT05633381). The skeletal system has not been characterized in patients treated with trabectedin; however, ~ 5% of primary soft tissue sarcomas metastasize to bone (43) and these patients can experience skeletal complications,

including fracture.(44) Taken together, evidence of fracture repair for patients taking these medications is lacking.

This study features clinical relevance by using two FDA-approved therapeutics to examine macrophages during stress fracture healing. We have shown, for the first time, macrophage infiltration into the stress fracture callus site. Using PTH and trabectedin as tools to impact macrophages, we were able to study the effect on callus formation and observe a correlation between macrophages and bone callus volume. In summary, this work highlights the growing body of literature that supports the critical role of macrophages during bone healing.

Acknowledgements

The authors would like to thank our funding sources, including the National Institute of Dental and Craniofacial Research (F30DE028455), the National Cancer Institute (P01CA093900), the National Institute of Arthritis and Musculoskeletal and Skin Diseases (AR077539), the National Institute of Diabetes and Digestive and Kidney Diseases (R56DK053904) of the National Institutes of Health (NIH); and the Department of Defense (W81XWH-14-1-0408). We also appreciate the contributions of Michelle Lynch from the University of Michigan School of Dentistry MicroCT Core (funded in part by NIH/NCRR S10RR026475-01 and the NIAMS P30 AR069620 to Karl Jepsen, PI; David H. Kohn, Core Director) and the University of Michigan Consulting for Statistics, Computing, and Analytics Research (funded by the University of Michigan).

Role of Funding Sources:

Funding sources are listed under Acknowledgements and were not involved in the study design; collection, analysis, and interpretation of data; writing of the report; and the decision to submit the article for publication.

References

1. LeBlanc AD, Spector ER, Evans HJ, and Sibonga JD (2007) Skeletal responses to space flight and the bed rest analog: a review. J Musculoskelet Neuronal Interact 7, 33–47 [PubMed: 17396004]
2. Kohrt WM, Bloomfield SA, Little KD, Nelson ME, Yingling VR, and American College of Sports, M. (2004) American College of Sports Medicine position stand: physical activity and bone health. Med Sci Sports Exerc 36, 1985–1996 [PubMed: 15514517]
3. Goolsby MA, and Boniquit N (2017) Bone health in athletes. Sports Health 9, 108–117 [PubMed: 27821574]
4. Burr DB, Forwood MR, Fyhrie DP, Martin RB, Schaffler MB, and Turner CH (1997) Bone microdamage and skeletal fragility in osteoporotic and stress fractures. J Bone Miner Res 12, 6–15 [PubMed: 9240720]
5. Bennell KL, and Brukner PD (1997) Epidemiology and site specificity of stress fractures. Clin Sports Med 16, 179–196 [PubMed: 9238304]
6. Cosman F, Ruffing J, Zion M, Uhorchak J, Ralston S, Tendy S, McGuigan FE, Lindsay R, and Nieves J (2013) Determinants of stress fracture risk in United States Military Academy cadets. Bone 55, 359–366 [PubMed: 23624291]
7. Fredericson M, Jennings F, Beaulieu C, and Matheson GO (2006) Stress fractures in athletes. Top Magn Reson Imaging 17, 309–325 [PubMed: 17414993]
8. Bahney CS, Zondervan RL, Allison P, Theologis A, Ashley JW, Ahn J, Miclau T, Marcucio RS, and Hankenson KD (2019) Cellular biology of fracture healing. J Orthop Res 37, 35–50 [PubMed: 30370699]
9. Claes L, Recknagel S, and Ignatius A (2012) Fracture healing under healthy and inflammatory conditions. Nat Rev Rheumatol 8, 133–143 [PubMed: 22293759]
10. Maruyama M, Rhee C, Utsunomiya T, Zhang N, Ueno M, Yao Z, and Goodman SB (2020) Modulation of the inflammatory response and bone healing. Front Endocrinol (Lausanne) 11, 386 [PubMed: 32655495]

11. Yahara Y, Ma X, Gracia L, and Alman BA (2021) Monocyte/macrophage lineage cells from fetal erythromyeloid progenitors orchestrate bone remodeling and repair. Front Cell Dev Biol 9, 622035 [PubMed: 33614650]
12. Raggatt LJ, Wullschleger ME, Alexander KA, Wu AC, Millard SM, Kaur S, Maugham ML, Gregory LS, Steck R, and Pettit AR (2014) Fracture healing via periosteal callus formation requires macrophages for both initiation and progression of early endochondral ossification. Am J Pathol 184, 3192–3204 [PubMed: 25285719]
13. Batoon L, Millard SM, Wullschleger ME, Preda C, Wu AC, Kaur S, Tseng HW, Hume DA, Levesque JP, Raggatt LJ, and Pettit AR (2019) CD169(+) macrophages are critical for osteoblast maintenance and promote intramembranous and endochondral ossification during bone repair. Biomaterials 196, 51–66 [PubMed: 29107337]
14. Alexander KA, Chang MK, Maylin ER, Kohler T, Muller R, Wu AC, Van Rooijen N, Sweet MJ, Hume DA, Raggatt LJ, and Pettit AR (2011) Osteal macrophages promote in vivo intramembranous bone healing in a mouse tibial injury model. J Bone Miner Res 26, 1517–1532 [PubMed: 21305607]
15. Uthgenannt BA, Kramer MH, Hwu JA, Wopenka B, and Silva MJ (2007) Skeletal self-repair: stress fracture healing by rapid formation and densification of woven bone. J Bone Miner Res 22, 1548–1556 [PubMed: 17576168]
16. Martinez MD, Schmid GJ, McKenzie JA, Ornitz DM, and Silva MJ (2010) Healing of non-displaced fractures produced by fatigue loading of the mouse ulna. Bone 46, 1604–1612 [PubMed: 20215063]
17. Wu AC, Morrison NA, Kelly WL, and Forwood MR (2013) MCP-1 expression is specifically regulated during activation of skeletal repair and remodeling. Calcif Tissue Int 92, 566–575 [PubMed: 23460341]
18. Zweifler LE, Koh AJ, Daignault-Newton S, and McCauley LK (2021) Anabolic actions of PTH in murine models: two decades of insights. J Bone Miner Res 36, 1979–1998 [PubMed: 34101904]
19. Cho SW, Soki FN, Koh AJ, Eber MR, Entezami P, Park SI, van Rooijen N, and McCauley LK (2014) Osteal macrophages support physiologic skeletal remodeling and anabolic actions of parathyroid hormone in bone. Proc Natl Acad Sci U S A 111, 1545–1550 [PubMed: 24406853]
20. Germano G, Frapolli R, Belgiovine C, Anselmo A, Pesce S, Liguori M, Erba E, Uboldi S, Zucchetti M, Pasqualini F, Nebuloni M, van Rooijen N, Mortarini R, Beltrame L, Marchini S, Fuso Nerini I, Sanfilippo R, Casali PG, Pilotti S, Galmarini CM, Anichini A, Mantovani A, D'Incalci M, and Allavena P (2013) Role of macrophage targeting in the antitumor activity of trabectedin. Cancer Cell 23, 249–262 [PubMed: 23410977]
21. Sinder BP, Zweifler L, Koh AJ, Michalski MN, Hofbauer LC, Aguirre JI, Roca H, and McCauley LK (2017) Bone mass is compromised by the chemotherapeutic trabectedin in association with effects on osteoblasts and macrophage efferocytosis. J Bone Miner Res 32, 2116–2127 [PubMed: 28600866]
22. Jones JD, Sinder BP, Paige D, Soki FN, Koh AJ, Thiele S, Shiozawa Y, Hofbauer LC, Daignault S, Roca H, and McCauley LK (2019) Trabectedin reduces skeletal prostate cancer tumor size in association with effects on M2 macrophages and efferocytosis. Neoplasia 21, 172–184 [PubMed: 30591422]
23. Sloan AV, Martin JR, Li S, and Li J (2010) Parathyroid hormone and bisphosphonate have opposite effects on stress fracture repair. Bone 47, 235–240 [PubMed: 20580684]
24. Hong H, Song T, Liu Y, Li J, Jiang Q, Song Q, and Deng Z (2019) The effectiveness and safety of parathyroid hormone in fracture healing: a meta-analysis. Clinics (Sao Paulo) 74, e800 [PubMed: 31038646]
25. Wu CA, Pettit AR, Toulson S, Grondahl L, Mackie EJ, and Cassady AI (2009) Responses in vivo to purified poly(3-hydroxybutyrate-co-3-hydroxyvalerate) implanted in a murine tibial defect model. J Biomed Mater Res A 91, 845–854 [PubMed: 19065568]
26. Colnot C (2009) Skeletal cell fate decisions within periosteum and bone marrow during bone regeneration. J Bone Miner Res 24, 274–282 [PubMed: 18847330]

27. Monfoulet L, Rabier B, Chassande O, and Fricain JC (2010) Drilled hole defects in mouse femur as models of intramembranous cortical and cancellous bone regeneration. Calcif Tissue Int 86, 72–81 [PubMed: 19953233]
28. Clark D, Brazina S, Yang F, Hu D, Hsieh CL, Niemi EC, Miclau T, Nakamura MC, and Marcucio R (2020) Age-related changes to macrophages are detrimental to fracture healing in mice. Aging Cell 19, e13112 [PubMed: 32096907]
29. Alexander KA, Raggatt LJ, Millard S, Batoon L, Chiu-Ku Wu A, Chang MK, Hume DA, and Pettit AR (2017) Resting and injury-induced inflamed periosteum contain multiple macrophage subsets that are located at sites of bone growth and regeneration. Immunol Cell Biol 95, 7–16 [PubMed: 27553584]
30. Coates BA, McKenzie JA, Buettmann EG, Liu X, Gontarz PM, Zhang B, and Silva MJ (2019) Transcriptional profiling of intramembranous and endochondral ossification after fracture in mice. Bone 127, 577–591 [PubMed: 31369916]
31. Mendoza-Reinoso V, Baek DY, Kurutz A, Rubin JR, Koh AJ, McCauley LK, and Roca H (2020) Unique pro-inflammatory response of macrophages during apoptotic cancer cell clearance. Cells 9, 429 [PubMed: 32059476]
32. Schlundt C, El Khassawna T, Serra A, Dienelt A, Wendler S, Schell H, van Rooijen N, Radbruch A, Lucius R, Hartmann S, Duda GN, and Schmidt-Bleek K (2018) Macrophages in bone fracture healing: their essential role in endochondral ossification. Bone 106, 78–89 [PubMed: 26529389]
33. McCauley LK, Dalli J, Koh AJ, Chiang N, and Serhan CN (2014) Cutting edge: parathyroid hormone facilitates macrophage efferocytosis in bone marrow via proresolving mediators resolvin D1 and resolvin D2. J Immunol 193, 26–29 [PubMed: 24890726]
34. Verhaar HJ, and Lems WF (2010) PTH analogues and osteoporotic fractures. Expert Opin Biol Ther 10, 1387–1394 [PubMed: 20629581]
35. Lindsay R, Nieves J, Formica C, Henneman E, Woelfert L, Shen V, Dempster D, and Cosman F (1997) Randomised controlled study of effect of parathyroid hormone on vertebral-bone mass and fracture incidence among postmenopausal women on oestrogen with osteoporosis. Lancet 350, 550–555 [PubMed: 9284777]
36. Neer RM, Arnaud CD, Zanchetta JR, Prince R, Gaich GA, Reginster JY, Hodsman AB, Eriksen EF, Ish-Shalom S, Genant HK, Wang O, and Mitlak BH (2001) Effect of parathyroid hormone (1–34) on fractures and bone mineral density in postmenopausal women with osteoporosis. N Engl J Med 344, 1434–1441 [PubMed: 11346808]
37. Gariffo G, Bottai V, Falcinelli F, Di Sacco F, Cifali R, Troiano E, Capanna R, Mondanelli N, and Giannotti S (2023) Use of teriparatide in preventing delayed bone healing and nonunion: a multicentric study on a series of 20 patients. BMC Musculoskelet Disord 24, 184 [PubMed: 36906529]
38. Rana A, Aggarwal S, Bachhal V, Hooda A, Jindal K, and Dhillon MS (2021) Role of supplemental teriparatide therapy in management of osteoporotic intertrochanteric femur fractures. Int J Burns Trauma 11, 234–244 [PubMed: 34336390]
39. Babu S, Sandiford NA, and Vrahas M (2015) Use of Teriparatide to improve fracture healing: What is the evidence? World J Orthop 6, 457–461 [PubMed: 26191492]
40. Carswell AT, Eastman KG, Casey A, Hammond M, Shepstone L, Payerne E, Toms AP, MacKay JW, Swart AM, Greeves JP, and Fraser WD (2021) Teriparatide and stress fracture healing in young adults (RETURN - Research on Efficacy of Teriparatide Use in the Return of recruits to Normal duty): study protocol for a randomised controlled trial. Trials 22, 580 [PubMed: 34461961]
41. Grignani G, Le Cesne A, and Martin-Broto J (2022) Trabectedin as second-line treatment in advanced soft tissue sarcoma: quality of life and safety outcomes. Future Oncol 18, 13–22 [PubMed: 36200954]
42. Teplinsky E, and Herzog TJ (2017) The efficacy of trabectedin in treating ovarian cancer. Expert Opin Pharmacother 18, 313–323 [PubMed: 28140689]
43. Vezeridis MP, Moore R, and Karakousis CP (1983) Metastatic patterns in soft-tissue sarcomas. Arch Surg 118, 915–918 [PubMed: 6307217]

44. Tsuzuki S, Park SH, Eber MR, Peters CM, and Shiozawa Y (2016) Skeletal complications in cancer patients with bone metastases. Int J Urol 23, 825–832 [PubMed: 27488133]

Highlights:

- Macrophages are present during stress fracture repair.
- PTH enhances stress fracture callus macrophage infiltration and bone volume.
- Trabectedin reduces stress fracture callus macrophage number bone volume.
- Effects of trabectedin are resolved by co-administration with PTH.

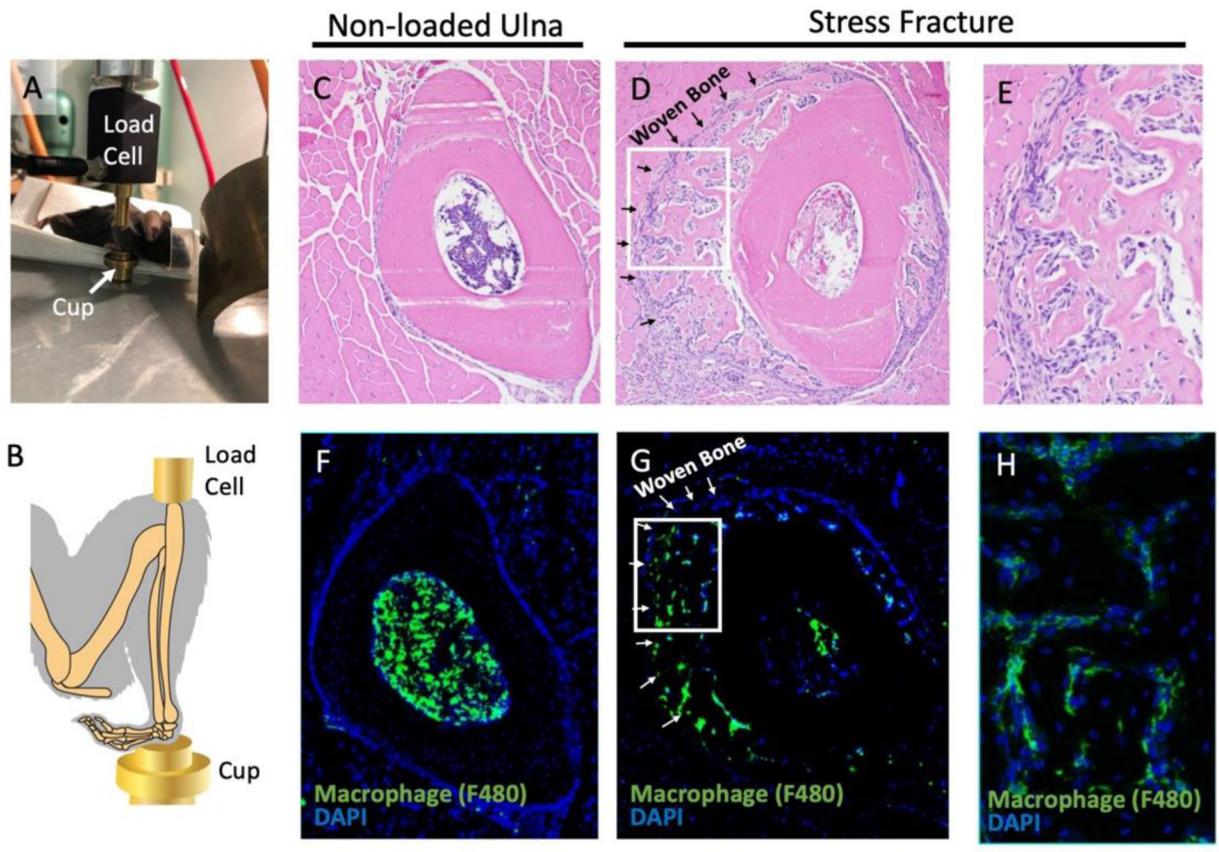

Figure 1. Repeated ulnar loading led to stress fracture and formation of a callus containing macrophages.

(A, B) The mouse was positioned with the ulna in a vertical position between the load cell and cup for stress fracture induction. (C-E) Hematoxylin and eosin staining was performed one week post injury in the ulna when non-loaded (C) or loaded to induce stress fracture (D,E). (F-H) Immunofluorescence with an F4/80 antibody was used to identify macrophages in an unloaded (F) and stress fracture callus (G, H). The boxes in panels D and G outline to the location of panels E and H, respectively. n=2

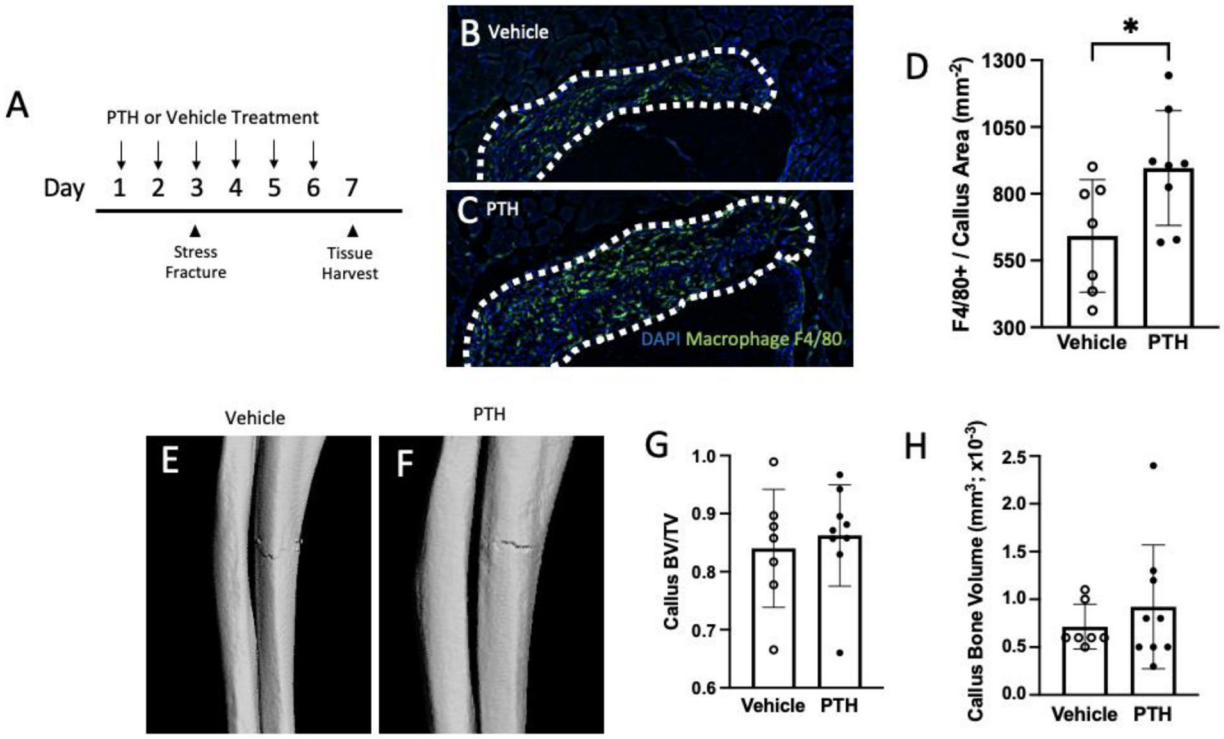

Figure 2. PTH treatment for six days, with stress fracture loading on day three, resulted in increased macrophage infiltration into the callus site.

(A) Experimental design with vehicle or PTH treatment started two days before loading the ulna for a stress fracture. Mice were euthanized 24 hours after the last treatment. (B,C) Sections stained with F4/80 antibody to quantify macrophage infiltration within the callus (outlined) with either vehicle or PTH treatment. (D) Quantification of F4/80 positive cell numbers per callus area. (E, F) Representative images (chosen by values closest to mean BV/TV) of stress fracture callus microCT renderings treated with either vehicle or PTH. (G, H) Callus bone volume per total volume (BV/TV) and callus bone volume analyzed by microCT are reported. Data was analyzed by T-tests using Prism software. *$p<0.05$, n=7–9/group

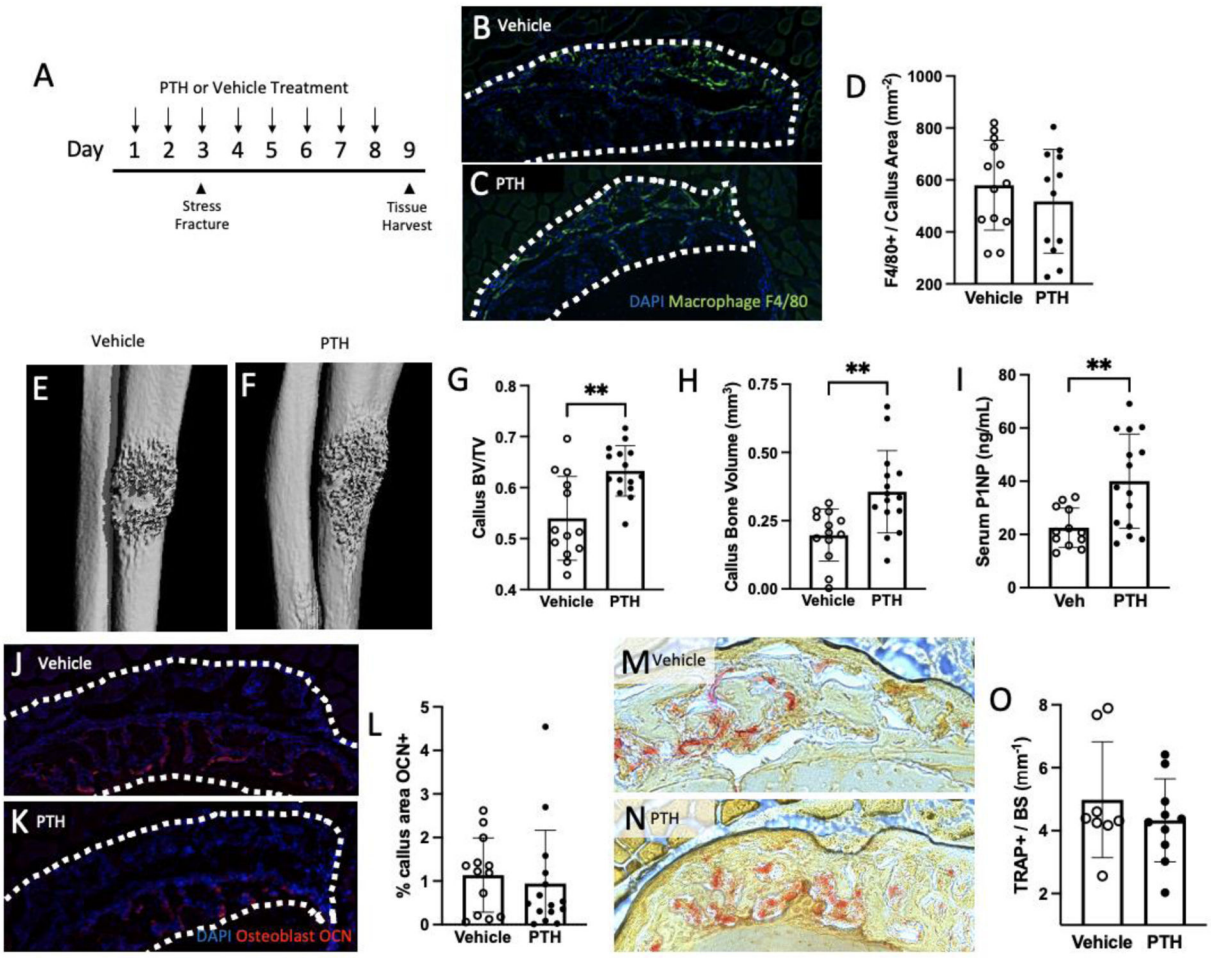

Figure 3. PTH treatment for eight days increased the callus size of hard callus formed in response to stress fracture.

(A) Experimental design with vehicle or PTH treatment starting two days before loading the ulna for a stress fracture. Mice were euthanized 24 hours after the last treatment. (B, C) Sections were stained with F4/80 antibody to quantify macrophage presence within the callus (outlined) with either vehicle or PTH treatment. (D) Quantification of F4/80 positive cells per callus area. (E, F) Representative images (chosen by values closest to the mean BV/TV) of stress fracture callus microCT renderings treated with either vehicle or PTH. (G, H) Callus bone volume per total volume (BV/TV) and callus bone volume analyzed by microCT are reported. (I) An ELISA was used to quantify the concentration of bone formation marker, P1NP in serum collected at the time of euthanasia. (J-L) Callus sections were stained with an antibody for osteocalcin (OCN; red) and quantified. Representative samples treated with vehicle (J) or PTH (K) are shown. (M-O) Osteoclasts were assessed with TRAP staining and reported as the number of TRAP positive cells per millimeter of bone surface with representative images shown for vehicle (M) and PTH (N) treatment. Data was analyzed by T-tests using Prism software. **p<0.01; n=8–15/group

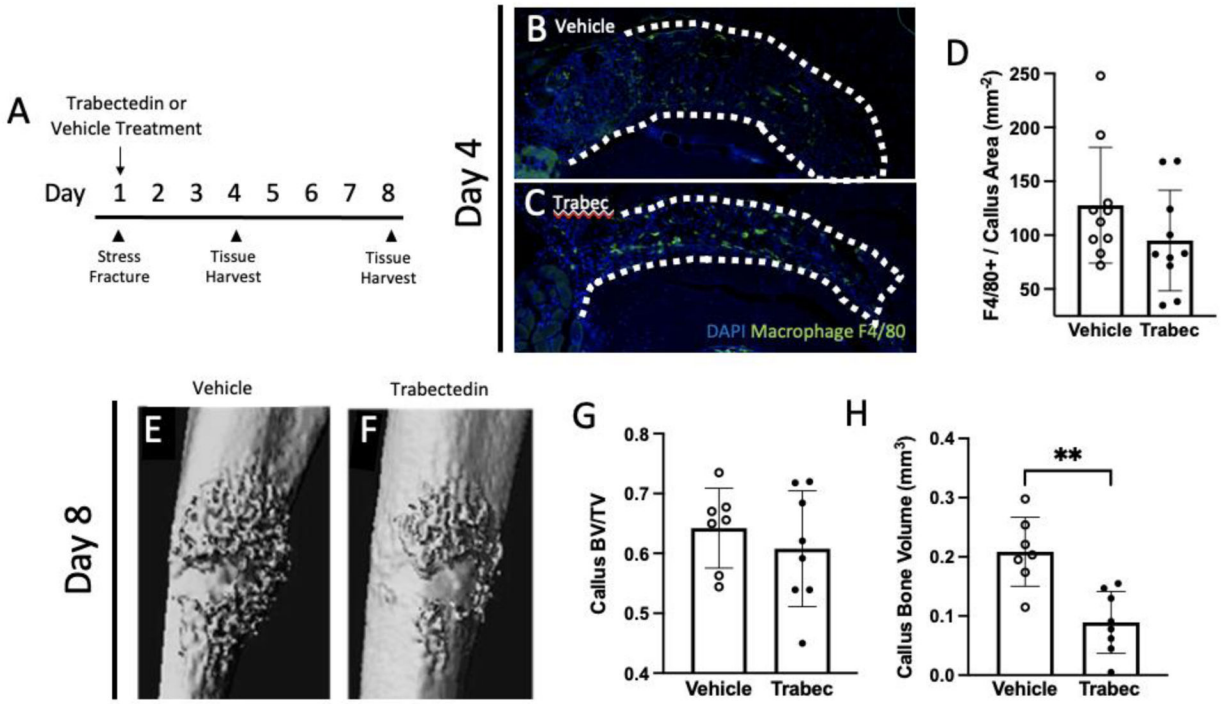

Figure 4. Trabectedin treatment decreased bone volume in a stress fracture callus.

(A) Experimental design with vehicle or trabectedin treatment starting on the day of stress fracture loading. Mice were euthanized on either day four or eight. (B, C) Samples from day four were stained with F4/80 to quantify macrophage infiltration with either vehicle or trabectedin treatment. (D) Quantification of the number of F4/80+ cells in the callus area following vehicle or trabectedin treatment. (E, F) Representative images (chosen by values closest to the mean BV/TV) of stress fracture callus microCT renderings treated with either vehicle or trabectedin. (G, H) Callus bone volume per total volume (BV/TV) and callus bone volume analyzed with microCT are reported. Data was analyzed by T-tests using Prism software. **p<0.01, trabec = trabectedin, n=7–10/group

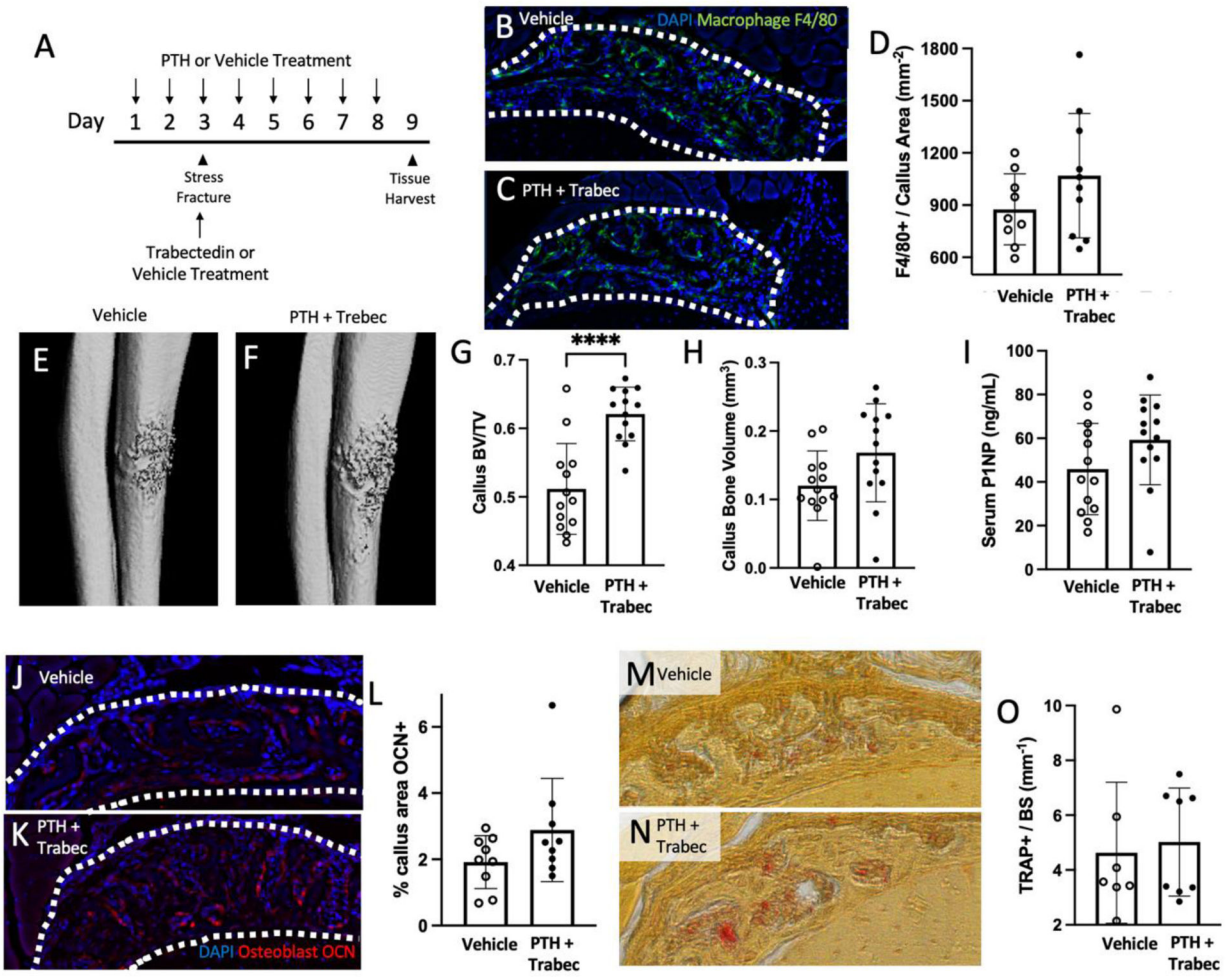

Figure 5. When treated with combination treatment of PTH and trabectedin, the callus is rescued from trabectedin alone.

(A) Experimental design with vehicle or PTH + trabectedin treatment following the same regime as previously described. Mice were euthanized 24 hours after the last PTH dose. (B, C) Sections were stained with F4/80 antibody to quantify macrophage presence within the callus (outlined) with either vehicle or PTH + trabec treatment. (D) Quantification of F4/80 positive cells per callus area. (E, F) Representative images of stress fracture callus microCT renderings treated with either vehicle or PTH + trabec. (G, H) Callus bone volume per total volume (BV/TV) and callus bone volume analyzed by microCT are reported. (I) An ELISA was used to quantify the concentration of bone formation marker, P1NP in serum collected at the time of euthanasia. (J-L) Callus sections were stained with an antibody for osteocalcin (OCN) and quantified. Representative samples treated with vehicle (J) or PTH + trabec (K) are shown. (M-O) Osteoclasts were assessed with TRAP staining and reported as the number of TRAP positive cells per millimeter of bone surface with representative images shown for vehicle (M) and PTH + trabec (N) treatment. Data was analyzed by T-tests using Prism software. **p<0.01; n=7–13/group; trabec = trabectedin